





## Adaptation of clinical isolates of *Klebsiella pneumoniae* to the combination of niclosamide with the efflux pump inhibitor phenyl-arginine- $\beta$ -naphthylamide (Pa $\beta$ N): co-resistance to antimicrobials

Olga Pacios<sup>1,2</sup>, Laura Fernández-García<sup>1,2</sup>, Inés Bleriot<sup>1,2</sup>, Lucia Blasco<sup>1,2</sup>, Antón Ambroa<sup>1,2</sup>, María López<sup>1,2,3</sup>, Concha Ortiz-Cartagena<sup>1,2</sup>, Manuel González de Aledo<sup>1</sup>, Felipe Fernández-Cuenca <sup>2,3,4</sup>, Jesús Oteo-Iglesias <sup>2,3,5</sup>, Álvaro Pascual <sup>2,3,4</sup>, Luis Martínez-Martínez<sup>2,3,6</sup>† and María Tomás <sup>1,2,3\*</sup>†

<sup>1</sup>Microbiology Department-Research Institute Biomedical A Coruña (INIBIC), Hospital A Coruña (CHUAC), University of A Coruña (UDC), A Coruña, Spain; <sup>2</sup>Study Group on Mechanisms of Action and Resistance to Antimicrobials (GEMARA) on behalf of the Spanish Society of Infectious Diseases and Clinical Microbiology (SEIMC); <sup>3</sup>Spanish Network for Research in Infectious Diseases (REIPI) and CIBER de Enfermedades Infecciosas (CIBERINFEC), Instituto de Salud Carlos III, Madrid, Spain; <sup>4</sup>Division of Infectious Diseases and Microbiology, University Hospital Virgen Macarena, Institute of Biomedicine of Sevilla (IBIS)/CSIC/University of Sevilla, Sevilla, Spain; <sup>5</sup>National Centre for Microbiology, Institute of Health Carlos III, 28029 Madrid, Spain; <sup>6</sup>UGC de Microbiología, Hospital Universitario Reina Sofía, Departamento de Química Agrícola, Edafología y Microbiología, Universidad de Córdoba, Instituto Maimónides de Investigación Biomédica de Córdoba (IMIBIC), Córdoba, Spain

\*Corresponding author. E-mail: MA.del.Mar.Tomas.Carmona@sergas.es

†These authors contributed equally to this work.

Received 25 October 2021; accepted 26 January 2022

**Objectives:** To search for new means of combatting carbapenemase-producing strains of *Klebsiella pneumoniae* by repurposing the anti-helminth drug niclosamide as an antimicrobial agent and combining it with the efflux pump inhibitor (EPI) phenyl-arginine- $\beta$ -naphthylamide (Pa $\beta$ N).

**Methods:** Niclosamide and Pa $\beta$ N MICs were determined for six clinical *K. pneumoniae* isolates harbouring different carbapenemases by broth microdilution and chequerboard assays. Time-kill curves in the presence of each drug alone and in combination were conducted. The viability of bacterial cells in the presence of repetitive exposures at 8 h to the treatment at the same concentration of niclosamide and/or Pa $\beta$ N (adapted isolates) was determined. The *acrAB-tolC* genes and their regulators were sequenced and quantitative RT-PCR was performed to assess whether the *acrA* gene was overexpressed in adapted isolates compared with non-adapted isolates. Finally, the MICs of several antimicrobials were determined for the adapted isolates.

**Results:** Niclosamide and Pa $\beta$ N had synergistic effects on the six isolates *in vitro*, but adaptation appeared when the treatment was applied to the medium every 8 h, with an increase of 6- to 12-fold in the MIC of Pa $\beta$ N. Sequencing revealed different mutations in the regulators of the tripartite AcrAB-TolC efflux pump (*ramR* and *acrR*) that may be responsible for the overexpression of the efflux pump and the adaptation to this combination. Co-resistance to different antimicrobials confirmed the overexpression of the AcrAB-TolC efflux pump.

**Conclusions:** Despite the synergistic effect that preliminary *in vitro* stages may suggest, the combinations of drugs and EPI may generate adapted phenotypes associated with antimicrobial resistance that must be taken into consideration.

### Introduction

Clinical failure is nowadays one of the most worrisome issues that we face daily, especially when treating antibiotic-resistant strains. Any new, successful drug used against acute and chronic microbial infections in the clinical setting could be correlated, to a greater or lesser extent, with resistance to it. In recent decades, few

new families of antibiotics have been discovered;<sup>1</sup> however, selection for resistance in clinical, veterinary and environmental settings has already occurred, as happens for every drug used routinely. In this context, the rescue of other types of FDA-approved drugs to treat microbial infections, especially those caused by MDR and adaptive bacteria, is necessary.<sup>2,3</sup> The strategy of finding new indications for drugs that already exist is known

as repositioning or drug-repurposing and has become increasingly popular lately.<sup>4–6</sup>

Niclosamide (2',5-dichloro-4'-nitrosalicylanilide) is an anti-helminth FDA-approved drug, belonging to the salicylanilide family, that has been used for 50 years against infections caused by parasites in humans and animals.<sup>7</sup> As an antibacterial molecule, niclosamide activity has been examined against many relevant pathogens and showed potent activity against the Gram-positive members of the ESKAPE pathogens, exclusively.<sup>8</sup> Moreover, many reports have found interesting results about its potential therapeutic use, *in vitro* and in *in vivo* models (*Galleria mellonella*,<sup>9</sup> *Caenorhabditis elegans*<sup>8</sup> and rodents<sup>10</sup>), highlighting: (i) niclosamide inhibited the growth of both vancomycin-resistant *Enterococcus faecium* (with MICs ranging from 1 to 8 mg/L) and *Staphylococcus aureus* (with an MIC value as low as 0.125 mg/L),<sup>8,11</sup> (ii) niclosamide inhibited *Pseudomonas aeruginosa* quorum sensing<sup>12</sup> and three toxins of *Clostridium difficile*,<sup>10</sup> in both cases exhibiting an anti-virulent role as an antibacterial molecule; (iii) niclosamide was repurposed as a surface coating to inhibit the biofilm of *S. aureus* resistant to methicillin and *Staphylococcus epidermidis* over hospital devices and its anti-biofilm activity was effective at concentrations as low as 10 mg/L,<sup>13</sup> and (iv) three different research groups have reported a synergistic effect between niclosamide and colistin on Gram-negative bacilli, even reverting the colistin resistance phenotype.<sup>14–16</sup>

Nevertheless, no relevant antibacterial effect of niclosamide alone on any Gram-negative strains has been assessed for now,<sup>13</sup> very likely due to two intrinsic mechanisms of resistance: the enzymatic nitroreduction carried out by nitroreductases and the activity of multidrug efflux pumps (such as AcrAB-TolC in *Escherichia coli*<sup>17</sup>). Copp *et al.*<sup>17</sup> found that, when the latter mechanism of resistance was inhibited, niclosamide became a potent antibiotic and dissipated the proton motive force, increasing oxidative stress and reducing ATP production, causing bacterial growth to stop. The authors hypothesized that niclosamide could have synergistic activity when combined with compounds that inhibit drug efflux. Thus, here we have combined

niclosamide with the well-characterized efflux pump inhibitor (EPI) phenyl-arginine-β-naphthylamide (PaβN) against clinical isolates of *Klebsiella pneumoniae*, so that the former could increase its intracellular concentration, while the tripartite efflux pump AcrAB-TolC is inhibited by PaβN, and therefore exhibit its bacteriostatic effect. As we observed adapted mutants following repetitive exposures of this combination, we sequenced the *acrAB* operon and *tolC* genes, encoding the AcrA periplasmic adapter protein, the AcrB membrane efflux transporter and the outer membrane channel TolC,<sup>18</sup> as well as the regulators of this system, such as *ramR*, *ramA* and *acrR*.<sup>19</sup> It has been described that *acrR* is the local repressor of the *acrAB* operon and mutations of it may cause the loss of its repressing function,<sup>20</sup> whereas *ramR* mutations can cause the overexpression of *ramA*, whose product RamA binds the promoter region of *acrAB* and activates the transcription of AcrAB-TolC. Thus, we also quantified the expression of *acrA* in adapted isolates (after three repetitive exposures to the treatment) by performing quantitative RT-PCR (qRT-PCR) and compared it with the expression in non-adapted isolates. Finally, the MICs of several antimicrobials (tigecycline, chloramphenicol, tetracycline, ciprofloxacin and imipenem) were determined to confirm the phenotypic co-resistance caused by the overexpression of the AcrAB-TolC efflux pump in the adapted isolates.

## Materials and methods

### *K. pneumoniae* clinical isolates

Six different isolates of *K. pneumoniae* belonging to different STs, previously determined by MLST, isolated from clinical samples and harbouring the most prevalent carbapenemase genes (OXA, VIM and KPC β-lactamases) were chosen (Figure 1a). The STs and carbapenemase β-lactamases had been determined by Esteban-Cantos *et al.*<sup>21</sup> The study pointed out that *K. pneumoniae* ST258 and ST15 are high-risk clones in the worldwide spread of carbapenemases (OXA-48, OXA-245, VIM-1, KPC-2 and KPC-3) and these were among the ones to be selected for analysis, together with a strain carrying no carbapenemase gene (K3325).

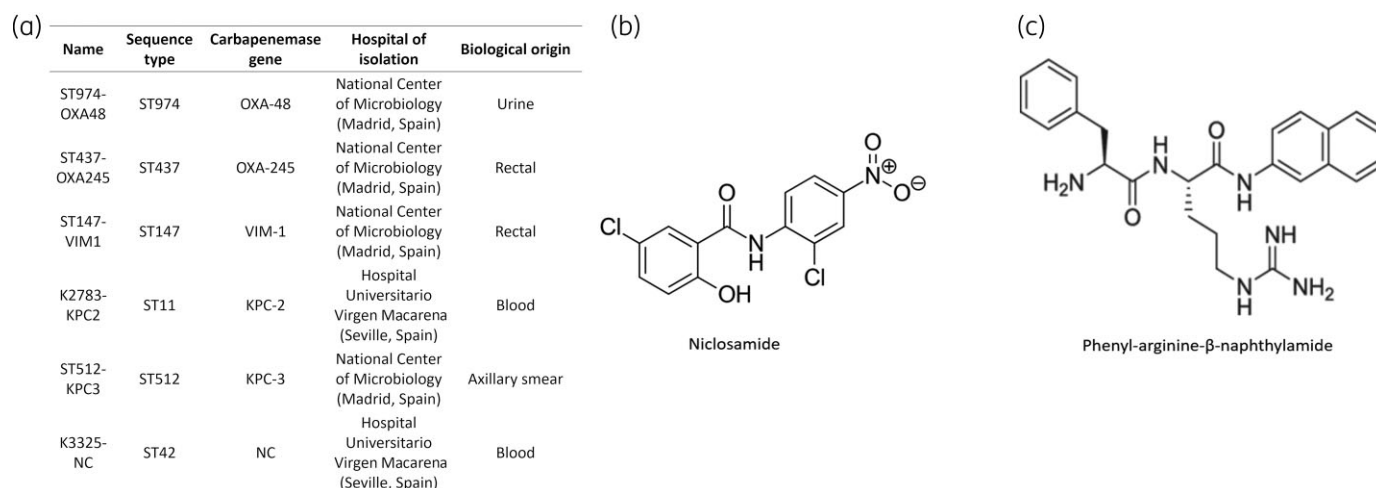


**Figure 1.** (a) Six heterogeneous clinical isolates, each one belonging to a different ST and carrying a different carbapenemase gene. NC, no carbapenemase. (b) FDA-approved anti-helminth niclosamide, belonging to the salicylanilide family. (c) Inhibitor of RND efflux pumps phenyl-arginine-β-naphthylamide (PaβN).

## Determination of the synergy in vitro between niclosamide and PaβN

### (a) Chequerboard assays

Niclosamide (Calbiochem®) and PaβN were purchased at Sigma-Aldrich® (Figure 1b and c). The MICs of both drugs individually were determined using a broth microdilution assay modified from established protocols.<sup>22</sup> Niclosamide (first diluted into DMSO) and PaβN (diluted into distilled water) were tested at the following ranges: 0.06–56.25 and 0.98–1000 mg/L, respectively. For the chequerboard assays, double dilutions of each drug (niclosamide along the x-axis and PaβN along the y-axis) were serially diluted in Mueller–Hinton broth, now at concentration ranges of 0.007–7.04 mg/L for niclosamide and 0.5–15.63 mg/L for PaβN, as these drugs in combination exhibited a stronger inhibitory activity. The six chosen clinical isolates of *K. pneumoniae* (Figure 1a) at a concentration of  $5 \times 10^5$  cfu/mL were added, whereas no bacteria were added to the negative controls. Plates were incubated for 16 h at 37°C and the MIC was the lowest concentration where no growth was visible. For calculation of the fractional inhibitory concentration index (FICI), a parameter that indicates the relationship established between two drugs, the following formulae were used:  $FIC_{\text{niclosamide}} = \text{MIC}_{\text{niclosamide}}$  in the presence of PaβN/ $\text{MIC}_{\text{niclosamide}}$ ,  $FIC_{\text{Pa}\beta\text{N}} = \text{MIC}_{\text{Pa}\beta\text{N}}$  in the presence of niclosamide/ $\text{MIC}_{\text{Pa}\beta\text{N}}$  and  $FICI = FIC_{\text{niclosamide}} + FIC_{\text{Pa}\beta\text{N}}$ .

### (b) Optical density (OD) growth curves and double-disc diffusion synergy assays

Isolated colonies of the six isolates of *K. pneumoniae* were inoculated in 5 mL of fresh LB broth, incubated overnight at 37°C and 180 rpm, then diluted 1:100 in LB broth and incubated in the presence of 3.5 mg/L niclosamide and/or 4 mg/L PaβN, defined after the chequerboard assays. The OD at a wavelength of 600 nm ( $OD_{600 \text{ nm}}$ ) was measured at 1 h intervals for 6 h. All experiments were performed in triplicate and statistically analysed using GraphPad v.6.

A double-disc diffusion assay was performed to verify this synergy in solid medium. Briefly, clinical isolates of *K. pneumoniae* were grown overnight and diluted 1:100 in LB broth. Aliquots (100 µL) of these dilutions were plated on Mueller–Hinton agar plates, where the antimicrobial susceptibility test discs (BD BBL™ Sensi-Disc™) were placed. Due to the low aqueous solubility of niclosamide, the discs containing niclosamide alone or with PaβN were imbibed into a solution of 1.8 mg/mL niclosamide alone or mixed with PaβN at 25 mg/mL for 2 s, based on previous works.<sup>13</sup> For discs where only PaβN was tested, 5 µL of the EPI at 25 mg/mL was added. Similarly, imipenem (10 µg, as a positive control) and distilled water and DMSO (5 µL, as negative controls) were included as controls (data not shown). To reveal the synergy in the confluence zone, niclosamide and PaβN discs were distanced 15 mm apart.

## Time–kill curves in the presence of niclosamide and PaβN

An isolated colony of each corresponding strain was inoculated overnight into 5 mL of LB broth and incubated at 37°C and 180 rpm, then diluted 1:100 in flasks containing 20 mL of LB broth. Niclosamide at a final concentration of 3.5 mg/L was also added alone or in combination with PaβN (4 mg/L). Every 8 h, cultures were centrifuged (4500 rpm, 15 min), washed with saline buffer, re-centrifuged, resuspended in fresh medium and niclosamide (3.5 mg/L) and/or PaβN (4 mg/L) were re-added to the same concentration. Bacterial concentrations ( $\log_{10}$  cfu/mL) were determined by counting the colonies present at 0, 8, 16 and 24 h post-treatment in LB agar after plating 100 µL of the cultures serially diluted. All experiments were performed in triplicate and statistically analysed using GraphPad v.6.

## Sequencing of *acrR*, *acrAB-tolC*, *ramR* and *ramA* (efflux pump genes) and qRT–PCR of *acrA*

*acrA*, *acrB* and *tolC* genes, as well as the regulators *acrR*, *ramA* and *ramR*, of the *K. pneumoniae* clinical strains that showed synergistic activity of the combination of niclosamide and PaβN were sequenced using the Sanger method at 0 h (control of non-adapted cells) and 24 h (adapted, as they have been exposed to three doses of the combination). Forward and reverse sequences were *de novo* assembled using Geneious Prime® 2021.2.2 and the identification of nucleotide changes was performed using the Blastn tool from the National Center for Biotechnology Information (NCBI). Nucleotide sequences were translated into protein sequences using the Expasy translate tool (<https://web.expasy.org/translate/>).

qRT–PCR was used to compare the expression of the *acrA* gene in adapted (24 h) and non-adapted (0 h) isolates. Lightcycler 480 RNA MasterHydrolysis Probe (Roche, Germany) and UPL Probes (Universal Probe Library–Roche, Germany) were used (Table S1, available as Supplementary data at JAC Online). All experiments were performed in duplicate from two independent RNA extractions (High Pure RNA Isolation Kit, following the manufacturer's instructions). For each strain, we normalized the expression of all genes relative to the *recA* housekeeping gene and calibrated the expression of *acrA* at 24 h relative to its expression in non-adapted strains. All the primers used in this work are shown in Table S1.

## Determination of the MICs of other antimicrobials

To phenotypically verify the overexpression of the AcrAB–TolC efflux pump in adapted strains, we determined the MICs for adapted strains in comparison with non-adapted strains of AcrAB–TolC substrates (tigecycline, chloramphenicol, tetracycline and ciprofloxacin), in the absence and the presence of PaβN. Imipenem (not a substrate of the efflux pump) was included as a control. We followed EUCAST methodology ([https://www.eucast.org/ast\\_of\\_bacteria/guidance\\_documents/](https://www.eucast.org/ast_of_bacteria/guidance_documents/)), double diluting each antibiotic in Mueller–Hinton broth and considering the MIC as the lowest concentration of compound that prevented visible growth after 16 h of incubation.

## Results

### Synergy of niclosamide in combination with the EPI PaβN

#### (a) Chequerboard assays

The MIC of niclosamide alone for every tested *K. pneumoniae* clinical isolate was found to be >56.25 mg/L, which is the solubility limit of this drug in aqueous growth media,<sup>17</sup> whereas the MIC of PaβN alone ranged from 500 to 1000 mg/L. Both values are in accordance with previous results.<sup>16,23</sup> Interestingly, the MIC of both drugs in combination for all the *K. pneumoniae* clinical isolates tested in the chequerboard assays decreased >64-fold in the case of niclosamide and >250-fold for the EPI PaβN (Table 1). The FICI parameter was calculated and synergistic values  $\leq 0.5$  were obtained for all the clinical strains tested in this study.<sup>24</sup>

#### (b) Synergistic studies in liquid and solid media

To assess how niclosamide and PaβN affect bacterial viability *in vitro*, we performed growth curves in liquid medium in which the  $OD_{600 \text{ nm}}$  was measured for 6 h at 1 h intervals in the presence of 3.5 mg/L niclosamide and 4 mg/L PaβN, the optimal concentrations found to inhibit the growth of every clinical strain tested (Figure 2, yellow squares). We observed a strong

**Table 1.** MICs of niclosamide and PaβN alone and in combination (chequerboard assays) and FICI values

| Bacterial strain | MIC of niclosamide (mg/L) | MIC of niclosamide in the presence of PaβN | FIC of niclosamide | MIC of PaβN (mg/L) | MIC of PaβN in the presence of niclosamide | FIC of PaβN | FICI   |
|------------------|---------------------------|--|--------------------|--------------------|--|-------------|--------|
| ST974-OXA48      | >56.25                    | 0.88                                       | 0.0156             | 500                | 3.91                                       | 0.0078      | 0.0235 |
| ST437-OXA245     | >56.25                    | 0.44                                       | 0.0078             | 500                | 3.91                                       | 0.0078      | 0.0156 |
| ST147-VIM1       | >56.25                    | 0.88                                       | 0.0156             | 1000               | 3.91                                       | 0.0039      | 0.0196 |
| K2783-KPC2       | >56.25                    | 0.88                                       | 0.0156             | 500                | 3.91                                       | 0.0078      | 0.0235 |
| ST512-KPC3       | >56.25                    | 1.76                                       | 0.0313             | 1000               | 3.91                                       | 0.0039      | 0.0352 |
| K3325-NC         | >56.25                    | 0.44                                       | 0.0078             | 500                | 3.91                                       | 0.0078      | 0.0156 |

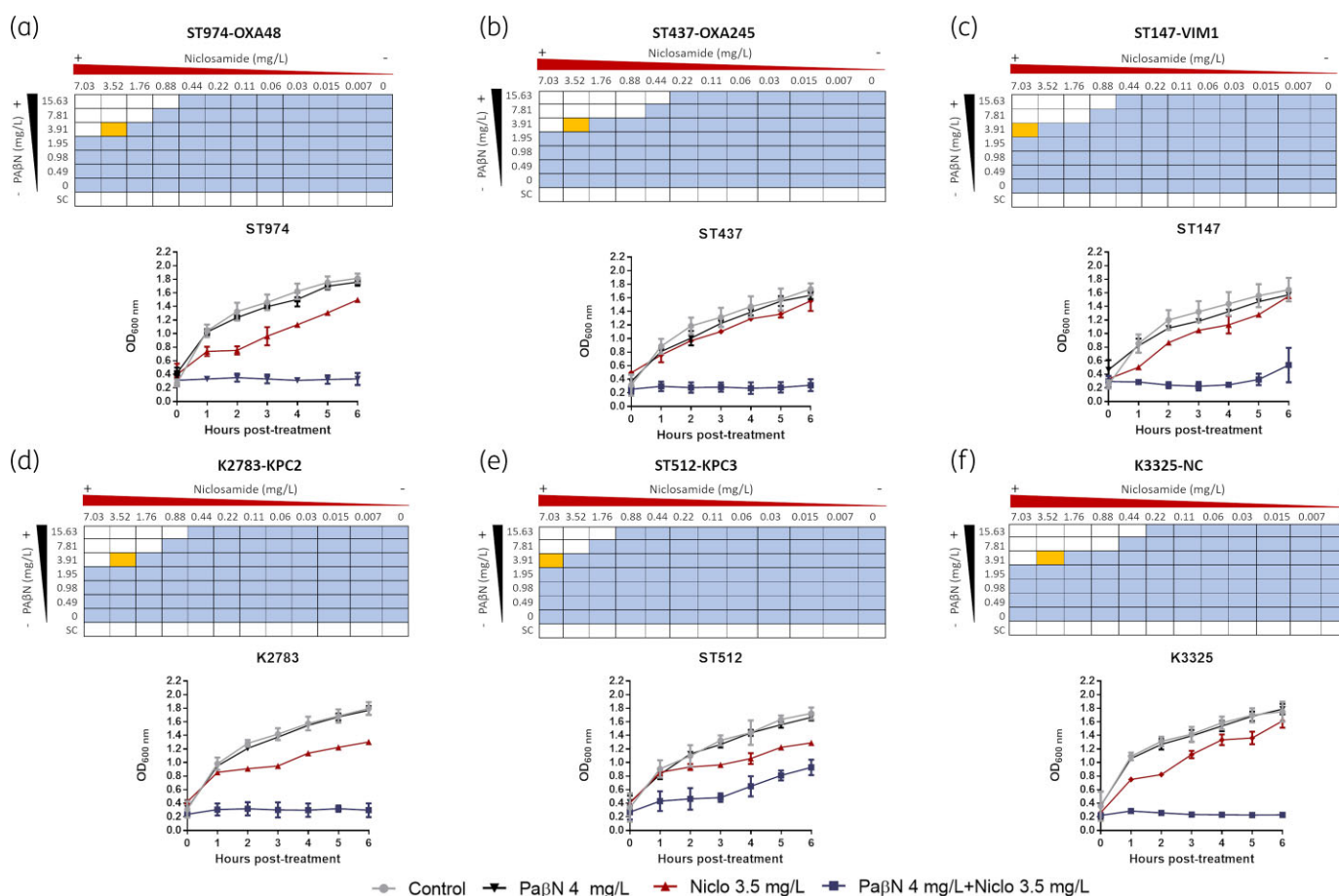


**Figure 2.** (a–f) Chequerboard assays and OD<sub>600 nm</sub> measurements of the six clinical isolates of *K. pneumoniae*. In the chequerboard plates, the white squares correspond to the wells where no growth was visible, whereas the blue squares correspond to turbid wells. Yellow squares indicate the well where the lowest concentrations of both drugs were enough to inhibit the growth of the tested clinical isolates. Niclo, niclosamide. This figure appears in colour in the online version of *JAC* and in black and white in the print version of *JAC*.

synergistic effect at all the timepoints for isolates ST974-OXA48, ST437-OXA245, K2783-KPC2 and K3325-NC, but ST147-VIM1 and ST512-KPC3 showed a slight regrowth in the presence of the combination, starting at 5 and 3 h post-treatment, respectively (Figure 2c and e). Globally, PaβN showed no antibacterial activity at the concentration tested and niclosamide alone exhibited a

very slight bacteriostatic effect, consistent with previous results.<sup>15,16</sup>

We also examined whether niclosamide in combination with PaβN was capable of inhibiting *K. pneumoniae* growth in solid medium using the double-disc diffusion synergy assay. We observed that the discs imbued with niclosamide or PaβN alone

were not able to inhibit the growth of any *K. pneumoniae* isolate (Figure 3). However, when discs were distanced 15 mm apart (Figure 3a, b, c, g, h and i), a clear zone of growth inhibition formed in the area where both drugs diffuse. Furthermore, we placed a niclosamide-imbibed disc and a Pa $\beta$ N-imbibed disc 25 mm apart (so no synergy was visible, as the diffusion of the drugs could not converge) and a disc imbibed into a combined solution of both agents (Pa $\beta$ N and niclosamide) and this latter was the only one that resulted in a clear zone of inhibition (Figure 3d, e, f, j, k and l).

### Phenotypic and molecular assays after repetitive exposures to niclosamide and Pa $\beta$ N

#### (a) Viability study: enumeration of cfu/mL

Considering the previous results, we wanted to assess how niclosamide and Pa $\beta$ N affect bacterial viability and if this parameter would be maintained at repetitive exposures of the combination. For this experiment, we chose four out of the initial six clinical isolates, discarding ST147-VIM1 and ST512-KPC3 due to their growth curves, which indicated emerging resistance (Figure 2).

Enumeration of cfu was performed after addition of the treatment every 8 h, in order to determine the viability of bacterial cultures. Consistent with what has been already observed,<sup>8</sup> we corroborated that niclosamide, when AcrAB-TolC was inhibited by Pa $\beta$ N, had a bacteriostatic effect on all of the tested isolates for the first 16 h of treatment (Figure 4a, c and d), except for ST437-OXA245 (Figure 4b), which showed a regrowth at 16 h (after two supplementations with the combination). At 24 h, the bacterial concentrations of every isolate reached the bacterial counts of the controls, suggesting an adapted phenotype to the combination.

#### (b) Phenotypic study: MIC determination for isolates exposed to 24 h of combination treatment

We determined the MIC of Pa $\beta$ N for each strain at 24 h, that is after three 8 h intervals of combined treatment, and compared this result with the MIC in the absence of previous exposure. We found that the MIC increased 6.25-fold in the case of ST974-OXA48 and ST437-OXA245 isolates and 12.5-fold for K2783-KPC2 and K3325 (Table 2), suggesting that the adapted phenotype to niclosamide and Pa $\beta$ N was a bacterial strategy to

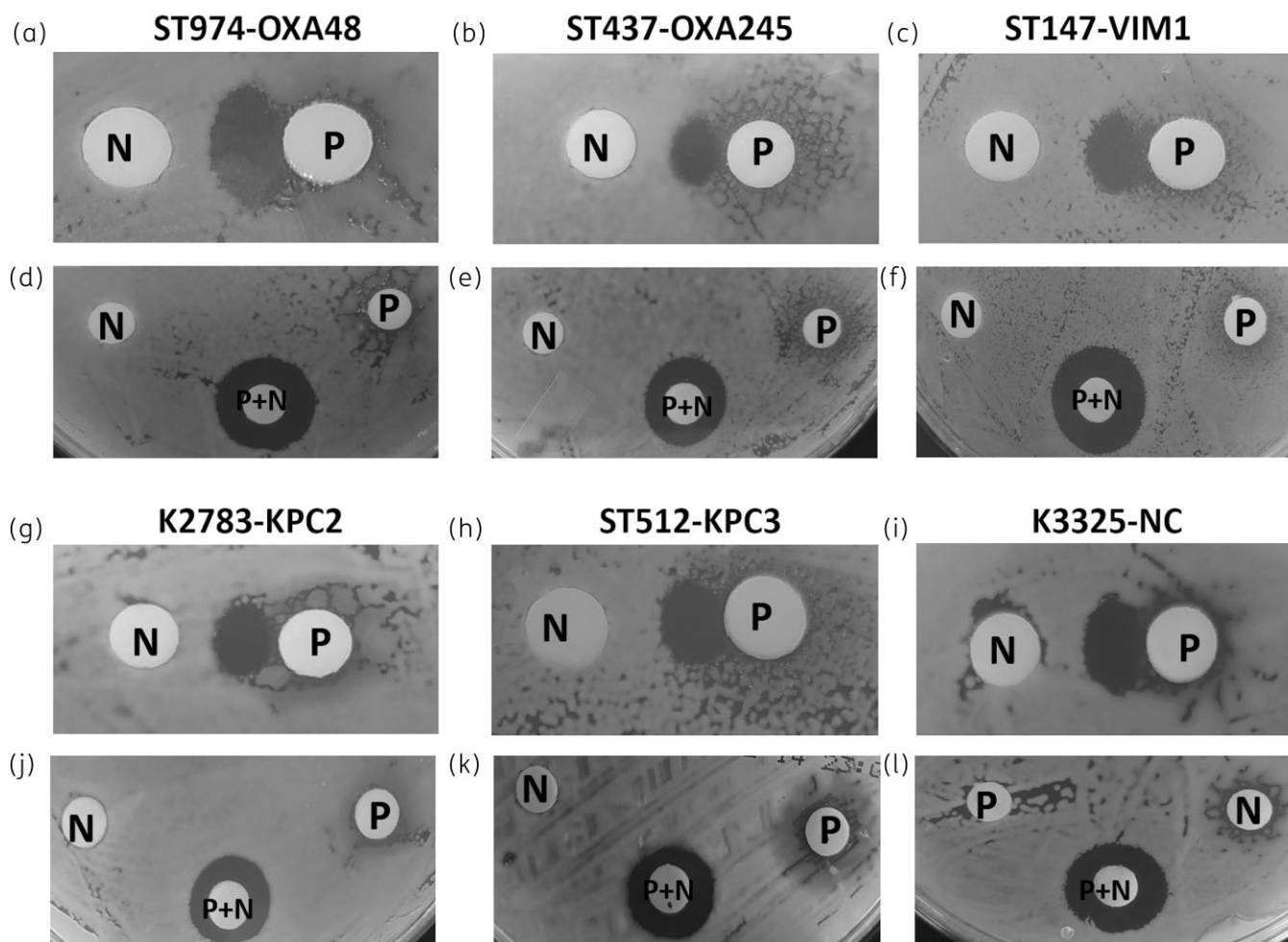


**Figure 3.** (a–l) Double-disc diffusion synergy test. N, niclosamide; P, Pa $\beta$ N; P+N, combination of Pa $\beta$ N and niclosamide.

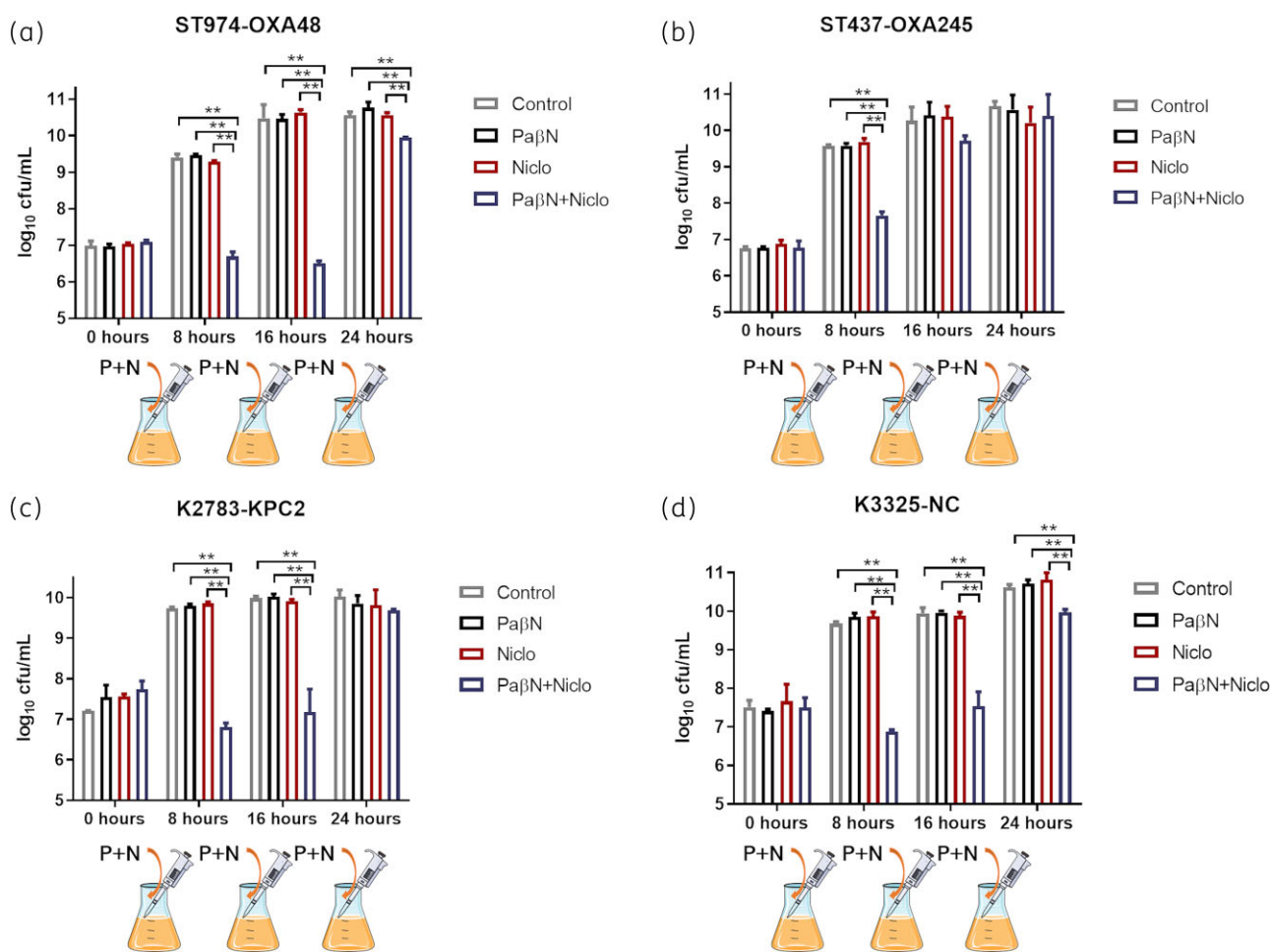


**Figure 4.** (a–d) Enumeration of viable colonies (cfu/mL) in the presence of no drug (control), EPI Pa $\beta$ N (4 mg/L), niclosamide alone (3.5 mg/L) or the combination of both agents at the aforementioned concentrations, re-added together with fresh LB medium at 8 h intervals. \*\* $P < 0.05$ . The absence of an asterisk means no statistically significant difference was found. ST147-VIM1 and ST512-KPC3 were not included in this experiment as they exhibited resistant growth curves in the presence of the combined treatment. Niclo, niclosamide; P+N, combination of Pa $\beta$ N and niclosamide. This figure appears in colour in the online version of *JAC* and in black and white in the print version of *JAC*.

better survive the period of treatment, typically with a weak dependence on the antibiotic concentration.<sup>25</sup>

(c) *Molecular study: analysis of *acrAB*-*tolC* mutations and relative expression of the *acrA* gene*

Since regrowth of every clinical strain tested was observed, we hypothesized that mutations in the regulator or the structural genes of the complex AcrAB-TolC were occurring, conferring the adapted phenotype.<sup>20,26</sup> Thus, we sequenced the genetic elements of the efflux pump AcrAB-TolC (*acrA*, *acrB* and *tolC*, as well as its regulators *ramR*, *ramA* and the local repressor *acrR*) for the clinical isolates at 0 and 24 h (Figure 5a).

We observed that one of the sequenced colonies of the ST437-OXA245 isolate carried a premature stop codon in *ramR*, at position 364, leading to a truncated RamR protein with 121 amino acids (lacking 73 residues compared with the wild-type protein), absent at 0 h. Furthermore, we found two mutations in *ramR* within the sequenced colonies corresponding to the

**Table 2.** Fold increase in the MIC of Pa $\beta$ N after continuous exposure of the bacterial cells to the combination treatment (ST147-VIM1 and ST512-KPC3 were not included in this experiment as they exhibited resistant growth curves in the presence of the combined treatment)

| Bacterial strain | MIC of Pa $\beta$ N (mg/L) | MIC of Pa $\beta$ N at 24 h (mg/L) | Fold increase in the MIC of Pa $\beta$ N |
|------------------|----------------------------|------------------------------------|--|
| ST974-OXA48      | 500                        | 3130                               | 6.25                                     |
| ST437-OXA245     | 500                        | 3130                               | 6.25                                     |
| K2783-KPC2       | 500                        | 6250                               | 12.5                                     |
| K3325-NC         | 500                        | 6250                               | 12.5                                     |

isolate ST974-OXA48, which were c.A344T and c.A394G, leading to the amino acid substitutions p.N115I and p.K131E, respectively. Similar point mutations have been described in *ramR* as well.<sup>27,28</sup> In this work, we have decided to name these mutations according to previously proposed rules, in which ‘c.’ stands for

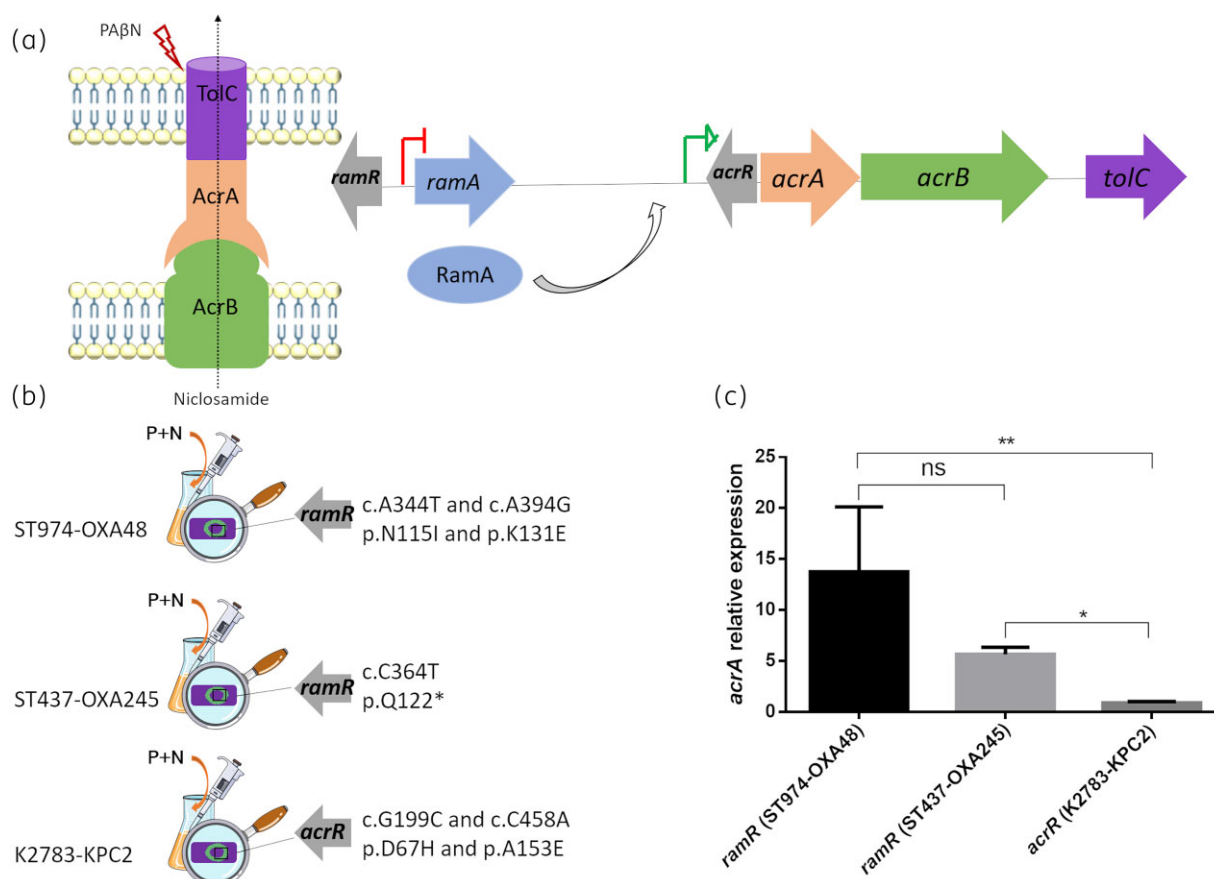


**Figure 5.** (a) Representation of the *acrAB* operon, the *tolC* gene, the local repressor *acrR*, the global regulator *ramR* and the *ramA* gene, encoding the RamA activator of *acrAB*. (b) Mutations found in the sequenced isolates. c., coding DNA; p., protein. The asterisk represents a premature stop codon. (c) Relative expression calculation after performing a qRT-PCR of the gene *acrA* in the adapted isolates (24 h of exposure to the treatment, with 8 h interval additions) compared with the same strains at 0 h (non-adapted). \* $P < 0.01$ ; \*\* $P < 0.001$ ; ns, no statistically significant difference was found. This figure appears in colour in the online version of JAC and in black and white in the print version of JAC.

coding DNA and ‘p.’ stands for protein (Figure 5b).<sup>29,30</sup> Concerning K2783-KPC2, we found some point mutations in the local repressor of the *acrAB* operon, named *acrR*, but only two led to missense mutations: the transversions c.G199C and c.C458A, which translate into p.D67H and p.A153E, respectively. No nucleotide changes were observed within the carbapenemase-free isolate K3325 or in the *ramA*, *tolC* or *acrAB* sequences of the four strains.

Concerning the relative expression of *acrA*, we observed an overexpression in the three adapted strains compared with the non-adapted strains, being significantly higher in the strains carrying *ramR* mutations than in the isolate where *acrR* was mutated (Figure 5c).

### Co-resistance to antimicrobials

To verify the overexpression of the AcrAB-TolC efflux pump in adapted strains (24 h) compared with the non-adapted strains (0 h), we determined the MICs of different substrates of this efflux pump, including glycines (tigecycline and tetracycline), a phenolic drug (chloramphenicol) and a fluoroquinolone

(ciprofloxacin), as well as the carbapenem imipenem, which is not an AcrAB-TolC substrate, in the absence and the presence of the EPI (Table 3). We observed that the MICs for the adapted isolates increased 2- to 8-fold compared with the non-adapted isolates for the two adapted strains where *ramR* was mutated and both in the absence and the presence of PaβN (Table 3), with higher increments in the isolate where RamA was truncated (ST437-OXA245; Figure 5b), even exceeding the breakpoint of chloramphenicol and becoming resistant to this drug ([https://www.eucast.org/ast\\_of\\_bacteria/guidance\\_documents/](https://www.eucast.org/ast_of_bacteria/guidance_documents/)). However, we observed a 1-fold increase (i.e. no increase) to 2-fold increase in the MICs of the tested antibiotics for K2783-KPC2 adapted to the treatment (24 h) compared with the non-adapted cells, suggesting that the *acrR* mutations found in K2783 adapted cells might not have an effect on the overexpression of AcrAB-TolC efflux pump as strong as the *ramR* mutations found in ST974-OXA48 and ST437-OXA245, which was already verified by qRT-PCR (Figure 4). We also observed increased MICs in the absence of EPI compared with the presence of this molecule for every drug except imipenem, which is not an AcrAB-TolC substrate<sup>31</sup> (Table 3).

**Table 3.** MICs of different antimicrobial substrates of the AcrAB-TolC efflux pump for adapted (24 h) and non-adapted clinical strains (ST147-VIM1 and ST512-KPC3) were not included in this experiment as they exhibited resistant growth curves in the presence of the combined treatment

| Bacterial strain    | MIC of tigecycline (mg/L) |             | MIC of chloramphenicol (mg/L) |            | MIC of tetracycline (mg/L) |    | MIC of ciprofloxacin (mg/L) |            | MIC of imipenem (mg/L) |             |
|---------------------|---------------------------|-------------|-------------------------------|------------|----------------------------|----|-----------------------------|------------|------------------------|-------------|
|                     | -P                        | +P          | -P                            | +P         | -P                         | +P | -P                          | +P         | -P                     | +P          |
| ST974-OXA48 (0 h)   | <b>3.04</b>               | <b>1.52</b> | 4                             | 0.5        | 2                          | 2  | <b>2</b>                    | 0.06       | <b>16</b>              | <b>16</b>   |
| ST974-OXA48 (24 h)  | <b>6.08</b>               | <b>3.04</b> | <b>16</b>                     | 2          | 16                         | 16 | <b>8</b>                    | 0.25       | > <b>32</b>            | <b>16</b>   |
| ST437-OXA245 (0 h)  | <b>3.04</b>               | <b>1.52</b> | 8                             | 2          | 4                          | 4  | > <b>8</b>                  | > <b>8</b> | <b>16</b>              | <b>32</b>   |
| ST437-OXA245 (24 h) | <b>12.1</b>               | <b>3.04</b> | > <b>32</b>                   | <b>16</b>  | 32                         | 8  | > <b>8</b>                  | > <b>8</b> | <b>8</b>               | <b>16</b>   |
| K2783-KPC2 (0 h)    | <b>3.04</b>               | <b>1.52</b> | > <b>128</b>                  | <b>128</b> | 4                          | 4  | > <b>8</b>                  | > <b>8</b> | > <b>32</b>            | > <b>32</b> |
| K2783-KPC2 (24 h)   | <b>3.04</b>               | <b>1.52</b> | > <b>128</b>                  | <b>128</b> | 8                          | 4  | > <b>8</b>                  | > <b>8</b> | > <b>32</b>            | > <b>32</b> |

-P and +P refer to the absence and the presence of Pa $\beta$ N, respectively.

Concentrations in bold are considered resistant according to the breakpoints of the EUCAST guidelines 2021.

## Discussion

In the current context of increasing resistance to antibiotics, carbapenemase-producing Enterobacteriaceae are of particular interest, as they have become resistant to almost every available antibiotic.<sup>32-34</sup> Among them, the rapid spread of carbapenemase-producing *K. pneumoniae* has provoked a public health crisis with serious consequences.<sup>34-36</sup> This pessimistic scenario makes the repurposing approach, in which molecules other than antibacterials are tested against MDR and opportunistic pathogens, suitable. Concerning niclosamide, which has been gathering strength lately due to its safety profile, its limitless repurposing capacity and the amount of information available, many researchers suggest that it could have a broad utility in combination therapies.<sup>8,11,15,16,37</sup>

In this work, niclosamide has been evaluated as a potential repurposed antibacterial agent against carbapenemase-producing *K. pneumoniae* isolates. Following Copp *et al.*<sup>17</sup> deductions, who described the mechanisms underlying the intrinsic resistance that Gram-negative bacteria exhibit towards niclosamide itself, we hypothesized that this anti-helminth molecule could have a synergistic activity in combination with the EPI Pa $\beta$ N. Regarding the FICI parameter calculated after performing the checkerboard assays, we observed a synergy between both molecules, with drastic reductions in the MIC of each drug when applied in the presence of the other. This synergistic effect was verified by OD<sub>600 nm</sub> growth curves (Figure 2) and we could also see a clear growth-inhibition zone in the Petri dishes where the clinical isolates were plated, but exclusively in the area where the diffusion of both molecules converged (Figure 3).

Nevertheless, despite these encouraging synergistic results, we observed that when the medium was supplemented every 8 h with the association of both drugs, this same combination generated an adapted phenotype (Figure 4). As the MIC of Pa $\beta$ N increased between 6- and 12-fold compared with the same isolates before continuous exposure of the treatment, we hypothesized that the regrowth of bacterial cells after repetitive and maintained additions of the combination was due to bacterial adaptation.<sup>38</sup>

To find a molecular basis for this phenotype, we sequenced the regulators of the efflux pump AcrAB-TolC (*ramR*, *ramA* and

*acrR*), as well as the genes encoding the proteins that constitute this complex, and we observed that no nucleotide mutation occurred inside the encoding regions of *tolC* or the *acrAB* operon; instead, a premature stop codon and point mutations appeared in the regulator sequences of *ramR* and *acrR* (Figure 5b). Premature stop codons in the global regulator *ramR* have already been described in other works, focusing on *K. pneumoniae*<sup>27,28,39</sup> and on *Salmonella enterica*.<sup>20,40</sup> As RamR is the repressor of *ramA*, which encodes the activator protein RamA that binds to the promoter region of *acrAB*, activating its transcription, we hypothesized that mutations in *ramR* can affect the repressing activity of RamR and, therefore, allow RamA to activate the transcription of the *acrAB* operon, leading to an overexpression of the efflux pump, which could explain the increments in the MIC.<sup>19,20,28,39-41</sup> We verified this overexpression by quantifying the expression of *acrA* relative to the non-adapted situation (in the absence of treatment, at 0 h) for the strains carrying *acrR* and *ramR* mutations and found a statistically significant increase in the overexpression of the efflux pump in the strains carrying the *ramR* mutations (Figure 5c).

It has been described that old antibiotics select their own resistance, but also resistance to more 'modern' drugs, which might be the case for repurposed agents, such as niclosamide.<sup>42</sup> We found that isolates adapted to niclosamide and Pa $\beta$ N were co-resistant to other antibiotics (i.e. substrates of AcrAB-TolC: tigecycline, chloramphenicol, tetracycline and ciprofloxacin). All in all, the EPI Pa $\beta$ N, even in combination therapy (with niclosamide), produced overexpression of the AcrAB efflux pump, associated with mutations in efflux pump regulators, generating an adapted phenotype, associated with co-resistance to several antimicrobials, in carbapenemase-producing *K. pneumoniae* clinical isolates.

## Funding

This study was funded by grant PI19/00878 awarded to M. Tomás within the State Plan for R+D+I 2013-2016 (National Plan for Scientific Research, Technological Development and Innovation 2008-2011) and co-financed by the ISCIII-Deputy General Directorate for Evaluation and Promotion of Research - European Regional Development Fund 'A way of Making Europe' and Instituto de Salud Carlos III FEDER, Spanish



Network for Research in Infectious Diseases (REIPI, RD16/0016/0001, RD16/0016/0006 and RD16/CIII/0004/0002) and by the Study Group on Mechanisms of Action and Resistance to Antimicrobials, GEMARA (SEIMC, <http://www.seimc.org/>). M. Tomás was financially supported by the Miguel Servet Research Programme (SERGAS and ISCIII). I. Bleriot was financially supported by the pFIS programme (ISCIII, FI20/00302). O. Pacios, L. Fernández-García and M. López were financially supported by the grants IN606A-2020/035, IN606B-2021/013 and IN606B-2018/008, respectively (GAIN, Xunta de Galicia).

## Transparency declarations

None to declare.

## Supplementary data

Table S1 is available as [Supplementary data](#) at JAC Online.

## References

- Hutchings MI, Truman AW, Wilkinson B. Antibiotics: past, present and future. *Curr Opin Microbiol* 2019; **51**: 72–80.
- Domalaon R, Ammeter D, Brizuela M et al. Repurposed antimicrobial combination therapy: tobramycin-ciprofloxacin hybrid augments activity of the anticancer drug mitomycin c against multidrug-resistant Gram-negative bacteria. *Front Microbiol* 2019; **10**: 1556.
- Farha MA, Brown ED. Drug repurposing for antimicrobial discovery. *Nat Microbiol* 2019; **4**: 565–77.
- Pacios O, Blasco L, Bleriot I et al. Strategies to combat multidrug-resistant and persistent infectious diseases. *Antibiotics (Basel)* 2020; **9**: 65.
- Chopra S, Torres-Ortiz M, Hokama L et al. Repurposing FDA-approved drugs to combat drug-resistant *Acinetobacter baumannii*. *J Antimicrob Chemother* 2010; **65**: 2598–601.
- Chopra S, Matsuyama K, Hutson C et al. Identification of antimicrobial activity among FDA-approved drugs for combating *Mycobacterium abscessus* and *Mycobacterium chelonae*. *J Antimicrob Chemother* 2011; **66**: 1533–6.
- Ditzel J, Schwartz M. Worm cure without tears. The effect of niclosamide on taeniasis saginata in man. *Acta Med Scand* 1967; **182**: 663–4.
- Rajamuthiah R, Fuchs BB, Conery AL et al. Repurposing salicylanilide anthelmintic drugs to combat drug resistant *Staphylococcus aureus*. *PLoS One* 2015; **10**: e0124595.
- Tharmalingam N, Port J, Castillo D et al. Repurposing the anthelmintic drug niclosamide to combat *Helicobacter pylori*. *Sci Rep* 2018; **8**: 3701.
- Tam J, Hamza T, Ma B et al. Host-targeted niclosamide inhibits *C. difficile* virulence and prevents disease in mice without disrupting the gut microbiota. *Nat Commun* 2018; **9**: 5233.
- Mohammad H, AbdelKhalek A, Abutaleb NS et al. Repurposing niclosamide for intestinal decolonization of vancomycin-resistant enterococci. *Int J Antimicrob Agents* 2018; **51**: 897–904.
- Imperi F, Massai F, Ramachandran Pillai C et al. New life for an old drug: the anthelmintic drug niclosamide inhibits *Pseudomonas aeruginosa* quorum sensing. *Antimicrob Agents Chemother* 2013; **57**: 996–1005.
- Gwisai T, Hollingsworth NR, Cowles S et al. Repurposing niclosamide as a versatile antimicrobial surface coating against device-associated, hospital-acquired bacterial infections. *Biomed Mater* 2017; **12**: 045010.
- Xu J, Pachón-Ibáñez ME, Cebrero-Cangueiro T et al. Discovery of niclosamide and its O-alkylamino-tethered derivatives as potent antibacterial agents against carbapenemase-producing and/or colistin resistant Enterobacteriaceae isolates. *Bioorg Med Chem Lett* 2019; **29**: 1399–402.
- Domalaon R, De Silva PM, Kumar A et al. The anthelmintic drug niclosamide synergizes with colistin and reverses colistin resistance in Gram-negative bacilli. *Antimicrob Agents Chemother* 2019; **63**: e02574–18.
- Ayerbe-Algaba R, Gil-Marqués ML, Jiménez-Mejías ME et al. Synergistic activity of niclosamide in combination with colistin against colistin-susceptible and colistin-resistant *Acinetobacter baumannii* and *Klebsiella pneumoniae*. *Front Cell Infect Microbiol* 2018; **8**: 348.
- Copp JN, Pletzer D, Brown AS et al. Mechanistic understanding enables the rational design of salicylanilide combination therapies for Gram-negative infections. *mBio* 2020; **11**: e02068–20.
- Du D, Wang Z, James NR et al. Structure of the AcrAB-TolC multidrug efflux pump. *Nature* 2014; **509**: 512–5.
- Ricci V, Busby SJ, Piddock LJ. Regulation of RamA by RamR in *Salmonella enterica* serovar Typhimurium: isolation of a RamR superrepressor. *Antimicrob Agents Chemother* 2012; **56**: 6037–40.
- Chen Y, Hu D, Zhang Q et al. Efflux pump overexpression contributes to tigecycline heteroresistance in *Salmonella enterica* serovar Typhimurium. *Front Cell Infect Microbiol* 2017; **7**: 37.
- Esteban-Cantos A, Aracil B, Bautista V et al. The carbapenemase-producing *Klebsiella pneumoniae* population is distinct and more clonal than the carbapenem-susceptible population. *Antimicrob Agents Chemother* 2017; **61**: e02520–16.
- Jorgensen JH, Ferraro MJ. Antimicrobial susceptibility testing: a review of general principles and contemporary practices. *Clin Infect Dis* 2009; **49**: 1749–55.
- Kvist M, Hancock V, Klemm P. Inactivation of efflux pumps abolishes bacterial biofilm formation. *Appl Environ Microbiol* 2008; **74**: 7376–82.
- Odds FC. Synergy, antagonism, and what the checkerboard puts between them. *J Antimicrob Chemother* 2003; **52**: 1.
- Bock LJ, Ferguson PM, Clarke M et al. *Pseudomonas aeruginosa* adapts to octenidine via a combination of efflux and membrane remodelling. *Commun Biol* 2021; **4**: 1058.
- Machado D, Antunes J, Simoes A et al. Contribution of efflux to colistin heteroresistance in a multidrug resistant *Acinetobacter baumannii* clinical isolate. *J Med Microbiol* 2018; **67**: 740–9.
- Li R, Han Y, Zhou Y et al. Tigecycline susceptibility and molecular resistance mechanisms among clinical *Klebsiella pneumoniae* strains isolated during non-tigecycline treatment. *Microb Drug Resist* 2017; **23**: 139–46.
- Hentschke M, Wolters M, Sobottka I et al. *ramR* mutations in clinical isolates of *Klebsiella pneumoniae* with reduced susceptibility to tigecycline. *Antimicrob Agents Chemother* 2010; **54**: 2720–3.
- Hall RM, Schwarz S. Resistance gene naming and numbering: is it a new gene or not? *J Antimicrob Chemother* 2016; **71**: 569–71.
- Ogino S, Gulley ML, den Dunnen JT et al. Standard mutation nomenclature in molecular diagnostics: practical and educational challenges. *J Mol Diagn* 2007; **9**: 1–6.
- Atzori A, Mallocci G, Cardamone F et al. Molecular interactions of carbapenem antibiotics with the multidrug efflux transporter AcrB of *Escherichia coli*. *Int J Mol Sci* 2020; **21**: 860.
- Tzouveleki LS, Markogiannakis A, Piperaki E et al. Treating infections caused by carbapenemase-producing Enterobacteriaceae. *Clin Microbiol Infect* 2014; **20**: 862–72.
- Nordmann P, Poirel L. The difficult-to-control spread of carbapenemase producers among Enterobacteriaceae worldwide. *Clin Microbiol Infect* 2014; **20**: 821–30.

- 34** Pitout JDD, Nordmann P, Poirel L. Carbapenemase-producing *Klebsiella pneumoniae*, a key pathogen set for global nosocomial dominance. *Antimicrob Agents Chemother* 2015; **59**: 5873–84.
- 35** Markogiannakis A, Tzouveleki LS, Psychogiou M et al. Confronting carbapenemase-producing *Klebsiella pneumoniae*. *Future Microbiol* 2013; **8**: 1147–61.
- 36** Pitout JDD, Peirano G, Kock MM et al. The global ascendancy of OXA-48-type carbapenemases. *Clin Microbiol Rev* 2019; **33**: e00102-19.
- 37** Fan X, Xu J, Files M et al. Dual activity of niclosamide to suppress replication of integrated HIV-1 and *Mycobacterium tuberculosis* (Beijing). *Tuberculosis (Edinb)* 2019; **116S**: S28–33.
- 38** Ciofu O, Tolker-Nielsen T. Tolerance and resistance of *Pseudomonas aeruginosa* biofilms to antimicrobial agents-how *P. aeruginosa* can escape antibiotics. *Front Microbiol* 2019; **10**: 913.
- 39** Xu Q, Sheng Z, Hao M et al. RamA upregulates multidrug resistance efflux pumps AcrAB and OqxAB in *Klebsiella pneumoniae*. *Int J Antimicrob Agents* 2021; **57**: 106251.
- 40** Abouzeed YM, Baucheron S, Cloeckaert A. *ramR* mutations involved in efflux-mediated multidrug resistance in *Salmonella enterica* serovar Typhimurium. *Antimicrob Agents Chemother* 2008; **52**: 2428–34.
- 41** Chiu S-K, Huang L-Y, Chen H et al. Roles of *ramR* and *tet(A)* mutations in conferring tigecycline resistance in carbapenem-resistant *Klebsiella pneumoniae* clinical isolates. *Antimicrob Agents Chemother* 2017; **61**: e00391-17.
- 42** Baquero F, Martínez JL, Novais Â et al. Allogeous selection of mutational collateral resistance: old drugs select for new resistance within antibiotic families. *Front Microbiol* 2021; **12**: 757833.